

Bio-inspired decision making in swarms under biases from stubborn robots, corrupted communication, and independent discovery

Raina Zakir^{1,*}, Timoteo Carletti², Marco Dorigo¹, and Andreagiovanni Reina^{3,4,*}

¹IRIDIA, Université Libre de Bruxelles, Brussels, Belgium

²Department of Mathematics and Namur Institute for Complex Systems, naXys, University of Namur, Namur, Belgium

³Centre for the Advanced Study of Collective Behaviour, Universität Konstanz, Konstanz, Germany

⁴Department of Collective Behaviour, Max Planck Institute of Animal Behavior, Konstanz, Germany

*raina.zakir@ulb.be; andreagiovanni.reina@uni-konstanz.de

ABSTRACT

Minimalistic robot swarms offer a scalable, robust, and cost-effective approach to performing complex tasks with the potential to transform applications in healthcare, disaster response, and environmental monitoring. However, coordinating such decentralised systems remains a fundamental challenge, particularly when robots are constrained in communication, computation, and memory. In our study, individual robots frequently make errors when sensing the environment, yet the swarm can rapidly and reliably reach consensus on the best among n discrete options. We compare two canonical mechanisms of opinion dynamics—direct-switch and cross-inhibition—which are simple yet effective rules for collective information processing observed in biological systems across scales, from neural populations to insect colonies. We generalise the existing mean-field models by considering asocial biases influencing the opinion dynamics. While swarms using direct-switch reliably select the best option in absence of asocial dynamics, their performance deteriorates once such biases are introduced, often resulting in decision deadlocks. In contrast, bio-inspired cross-inhibition enables faster, more cohesive, accurate, robust, and scalable decisions across a wide range of biased conditions. Our findings provide theoretical and practical insights into the coordination of minimal swarms and offer insights that extend to a broad class of decentralised decision-making systems in biology and engineering.

Introduction

Robot swarms are decentralised systems, typically composed of a large number of relatively simple robots, that coordinate to perform tasks or solve problems cooperatively. Robot swarms are meant to operate autonomously—without any centralised supervision—by using local interactions among the robots and with their surrounding environment¹. Simple, low-cost robots are well suited to constrained or hazardous environments, as they require minimal individual computation and can be produced in large numbers affordably². Enabling the swarm to make collective decisions is an essential requirement to achieve autonomy in such decentralised systems. Research in collective decision-making in robot swarms often draws inspiration from nature^{3,4},

where systems such as insect colonies and bird flocks follow simple local rules to reach rapid consensus without centralized control, for instance, when selecting the aggregation site^{5,6}, the direction of motion^{7,8}, or the shortest foraging path⁹. Potential applications that require minimal robot swarms to rapidly reach consensus include drug-delivery through bloodstream to the best tissue for payload release¹⁰, and assessment of fire affected infrastructure to identify the best locations to take containment actions¹¹.

In many real-world scenarios, robot swarms must select the best among multiple alternatives that vary in quality or cost—a task formalized as the best-of- n problem¹². Minimal swarms, composed of individuals with limited sensing and processing capabilities, can nevertheless overcome individual-level noise through repeated social interactions. Best-of- n decision-making processes are found in nature where biological collectives achieve robust, decentralised consensus by following simple local rules. For instance, ant and honeybee colonies routinely choose the best location to build their nest, with individual insects acting as noisy information-processing units¹³. Similarly, populations of neurons integrate noisy signals to guide behavioural responses¹⁴. Despite vast differences in scale and substrate, these systems rely on common mechanisms for information integration^{15–17}. Simple and effective, these mechanisms have also been adopted to design robot swarm behaviours for best-of- n decision-making^{6,18}. However, robustness to disturbances and asocial dynamics—such as robot malfunction, cyberattacks, or changing environments—is a crucial aspect for safe deployment of such systems that has not yet been fully addressed¹⁹.

In several biological systems, as well as in our robot swarm, agents can collectively select the best option through a repeated exchange of opinions. When agents communicate their opinion with a frequency proportional to how much they value it, the most frequently exchanged opinions diffuse quicker than others, leading to a consensus for the best option. However, how robots, insects, or neurons integrate information from peers determines the collective opinion dynamics, especially when they are biased by asocial dynamics. In this paper, we consider two alternative mechanisms commonly found in natural systems and implemented in swarm robotics: direct-switch and cross-inhibition (Figure 1A-B). The direct-switch mechanism (Figure 1A) periodically updates a robot's opinion by copying the one of a randomly chosen neighbour. The weighted voter model algorithm—that employs the direct-switch mechanism—has the advantage of being mathematically simple to analyse and computationally cheap to run on minimalistic systems, and has been widely used in robot swarms to solve the best-of- n problem^{20–24}. The cross-inhibition mechanism^{25–27} (Figure 1B)—inspired by the house-hunting behaviour in honeybees⁵—is another prominent collective decision-making mechanism of comparable simplicity to direct-switch. As a basic but effective mechanism, cross-inhibition can be found at every level of biological complexity for rapid consensus, including the cell cycle G2/M transition regulatory networks^{28,29}. Neuronal dynamics in the brains of decision-makers are often described with the leaky competing accumulator model, which follows remarkably similar information integration patterns to cross-inhibition^{14–16}. In contrast to direct-switch, if a robot utilizing the cross-inhibition mechanism receives a conflicting opinion from one of its neighbours (i.e., an opinion different from the current robot opinion), rather than directly copying it, it becomes uncommitted (or undecided). Only uncommitted robots copy and adopt other robots' opinion. Both mechanisms have been shown to enable individual units of the swarm—robots, animals, or neurons—to integrate social information and reach a consensus for the best alternative, even when only a slight majority correctly sense the environment^{15,21,27,30}. To meaningfully compare their performance, it is essential to study them under more realistic conditions, moving beyond idealized, noise-free models, as real-world swarms are inevitably subject to bias, noise, and external interference.

Our analysis focuses on three critical aspects of collective decision-making: decision speed, group cohesion, and accuracy,

which are key performance metrics in both robotic and natural systems^{21,31,32}. While decentralised systems have been extensively studied with regard to speed-accuracy trade-offs^{21,23,33}, speed-cohesion trade-offs have received comparatively little attention^{34,35}. We address this literature gap by conducting a systematic comparison of the two decision-making mechanisms—direct-switch and cross-inhibition—in terms of speed, cohesion, and accuracy under conditions involving asocial dynamics.

In our framework, asocial dynamics occur when robots update their opinion based on information that does not reflect the state of their peers. This may occur when robots combine social interactions with independent environmental exploration, or when they receive biased, distorted, or misleading information. While some forms of such asocial dynamics can be beneficial in controlled amounts^{36,37}, they more often impair collective performance by hindering consensus formation, prolonging indecision^{38–40}, or leading to suboptimal decisions^{41,42}. As illustrated in Figure 1C-E, we investigate three representative sources of asocial dynamics: (i) biased information spread by asocial robots that resist conforming to social pressure³⁹, (ii) corrupted communication due to message interception and alteration³⁷, and (iii) spontaneous opinion changes driven by self-sourced environmental information⁴³. Our study provides a mathematical formalisation showing that these seemingly distinct forms of asocial dynamics can be described by equivalent terms, enabling a unified treatment of their effects on collective decision-making.

Asocial dynamics can be categorised as unbiased—affecting all options equally—or biased towards certain alternatives. Previous work has studied the direct-switch and cross-inhibition mechanisms in several specific cases that our general model can describe in a unified compact form. These include theoretical and empirical analyses of swarms comprising unbiased social noise^{44–46} or two equally sized subgroups of zealots hindering, or sometimes facilitating, group consensus^{36,39,47–49}. Synergistic bias—where asocial dynamics favour the superior option—has mainly been studied in the form of self-sourcing (i.e., spontaneous discovery), where agents are more likely to independently encounter and commit to the best option^{15,22,25,27,43}. While it is often reasonable to assume that better options are closer or more abundant, and thus easier to find, this assumption does not always hold. Antagonistic bias—where asocial dynamics favour the inferior option—can also frequently arise in both natural and artificial systems. For instance, house-hunting insects⁵⁰ and robot swarms^{26,51} may face environments where the optimal choice is also the hardest to discover. Human groups⁵², as well as fish flocks⁵³ or ant colonies⁵⁴, can include minorities of stubborn individuals with strong biases that can sometimes take over the consensus⁵⁵. Artificial systems can also be under cyberattacks¹⁹ where communication is tampered^{37,56} or stubborn robots only support the inferior option^{41,42,47}. Our unified model is general enough to encompass most of these scenarios (see Supplementary Text 1 for an extended discussion).

In previous studies, we quantified the impact of specific forms of asocial dynamics on the opinion dynamics of groups by using direct-switch or cross-inhibition. Reina et al.³⁹ analysed, through mean-field analysis, the impact of introducing asocial agents, specifically zealots (individuals who are stubborn and never change their opinion), on both decision-making mechanisms, direct-switch and cross-inhibition. Zakir et al.³⁷ investigated the impact of another type of asocial dynamics, miscommunication among the robots, showing that, compared to the noise-free system, a certain level of asocial dynamics (in that case, manifested as communication errors) can increase the accuracy of the collective decisions, serving an important functional role in making collective decisions in robot swarms that use the cross-inhibition mechanism. Zakir et al.⁴³ also examined the impact of asocial dynamics caused by independent discovery, i.e., the probability of robots changing their opinion independently of social interaction by occasionally self-sourcing information from the environment. This self-sourcing

probability represents another form of opinion dynamics noise, which can have a critical impact on the collective dynamics, for example, preventing swarms using the direct-switch mechanism from reaching a consensus decision⁴³.

In this work, we study how asocial dynamics affect collective decision-making by combining mathematical modelling and stochastic swarm robotics simulations. We develop various deterministic ordinary differential equation (ODE) models to describe the swarm population dynamics at multiple levels of abstraction. A minimal model captures the core features of the direct-switch and cross-inhibition mechanisms, by enabling analytical insight and generalisation across disciplines. A second, more detailed model is tailored to our robotic scenario of collective perception, by allowing for quantitative comparisons with experimental data. To account for stochastic and finite-size effects, we define a microscopic model rooted on the use of a chemical-like reaction network simulated via the Gillespie algorithm⁵⁷, alongside realistic simulations of autonomous robots collectively sensing their environment⁴³. In our multiscale analysis, we show that different types of asocial influences—stubborn agents, corrupted communication, and independent information discovery—can be captured by mathematically equivalent terms. This unified formulation enables generalised reasoning about biased opinion dynamics in a wide class of distributed systems and makes possible the systematic comparison of decision-making mechanisms under diverse asocial conditions, spanning the full spectrum from synergistic to antagonistic. Finally, the bio-inspired nature of the mechanisms we study offers insights into decision-making trade-offs in natural systems, including insect colonies and neural assemblies.

Results

Equivalence of asocial dynamics

In the proposed framework, asocial dynamics can arise from any of the three factors illustrated in Figure 1. Rather than reading a message from a cooperative (social) peer, a robot may instead (i) interact with a zealot—an agent persistently favouring one option^{39,41} (Fig. 1C); (ii) self-source information from the environment, independently of social cues⁴³ (Fig. 1D); or (iii) receive a corrupted message due to a man-in-the-middle (MITM) attack that intercepts and alters communication³⁷ (Fig. 1E).

We generalise distinct forms of asocial dynamics by modelling them as variants of a single underlying mechanism that occurs with probability η at each opinion update. According to the decision-making algorithms, a robot updates its opinion by sampling a representative message from the social population; however, this event occurs only with probability $1 - \eta$ due to the presence of asocial dynamics (see right branch in the scheme of Fig. 2A). Conversely, with probability η (left branch in Fig. 2A), the robot updates its opinion using asocial information: a message from a zealot, a corrupted message, or an independently sourced opinion.

Any type of asocial dynamics can be biased towards either option. In a best-of-2 problem with options A and B, we define $\eta_a \in [0, 1]$ and $\eta_b = 1 - \eta_a$ as the biases of asocial information toward option A and B, respectively, meaning that on average, η_a of the asocial updates provide information in favour of A, and η_b in favour of B. More concretely, when z zealots are present, $\eta = z/N$ is the probability of interacting with a zealot, and $\eta_a = z_a/z$, $\eta_b = z_b/z$ represent the proportions of zealots favouring each option ($z_a + z_b = z$). In the case of MITM attacks, η is the probability of receiving a corrupted message, while η_a and η_b capture how often messages are altered to support option A or B. For self-sourcing, η is the probability that a robot uses environmental information rather than social input, and η_a , η_b represent how likely the robot is to independently discover evidence in favour of A or B—that is, how easily each option can be found in the environment. Although the interpretations differ across these cases, all three events involve updating the robot opinion based on biased information rather

than representative social input from the population.

This unified formulation simplifies the analysis of the mean-field models and enables systematic exploration of the parameter space defined by η and η_a . In the ODE models, opinion changes are the result from two concurrent processes: the decision-making mechanisms—defined by direct-switch (weighted voter model) or cross-inhibition—and biased asocial events, which act as a constant biased ‘opinion field’. This abstraction allows experimental results to generalise across contexts: the same effect can be achieved by modifying the number of zealots, altering the rate of message corruption, or adjusting environmental features that affect independent discovery of options (see Methods and Supplementary Text 3).

Collective perception with a minimalistic robot swarm

We employ the investigated decentralised decision-making mechanisms to enable efficient collective perception in a minimalistic robot swarm. As illustrated by the finite state machines in Figure 1A-B, each robot can be in one of three states depending on its opinion: committed to option A (state A), committed to option B (state B), or uncommitted (state U). Committed robots broadcast their opinion to nearby peers, while uncommitted robots remain silent. In both direct-switch and cross-inhibition mechanisms, robots periodically read a message from a randomly selected neighbour and update their opinion accordingly. The decision diagram in Figure 2A describes how a robot currently committed to option A decides whether to retain or change its opinion. These state transitions can also be modelled as chemical-like reaction networks (Figure 2B), where opinion changes are described by reaction rates. For the cross-inhibition mechanism, we consider two types of asocial dynamics: after an asocial event (e.g., self-sourcing), robots either become uncommitted (type 1) or switch directly to the new opinion (type 2).

Figures 1A-B and 2 present the basic algorithmic models which, thanks to their simplicity, allow generalisation of insights across domains and applications, from robotics to natural collectives. However, when implementing these basic algorithms in physical robots, certain adaptations are required to meet the constraints of real-world applications. A critical aspect regards quality estimation. Sampling the environment to determine the option quality can require time, either because options may correspond to specific spatial locations that robots need to visit^{21,22}, or to distributed environmental features that the robots need to repeatedly sample^{58,59}. Following earlier approaches^{20,21,43}, we extend the basic decision-making algorithms by introducing two alternating phases: exploration and dissemination (see finite state machine in Figure 3A and Supplementary Text 2). During exploration, a robot estimates the quality of its currently supported option; during dissemination, it broadcasts its opinion to neighbours.

Our robots are minimalistic, with extremely limited computation, memory, and communication capabilities. Like house-hunting insects^{5,15}, each robot only stores and communicates information about one option. The robot estimates can be extremely noisy, e.g., compare the true quality (yellow point) with the robot measurements (black points) in Figure 3C. Despite the individual robot limitations, by disseminating an opinion for a time proportional to the estimated quality, the swarm collectively amplifies small differences in population opinions and reliably makes consensus decisions on the best option.

In our collective perception task, robots must choose between two environmental features, modelled as different floor tile colours (red for option A and blue for option B—see Figure 3B). As they move, robots collect noisy measurements of local quality. Occasionally, a robot disregards social input and instead self-sources information from the environment by switching its commitment to the option associated with the tile it locally senses. Therefore, the proportion of tile colours defines the self-sourcing bias.

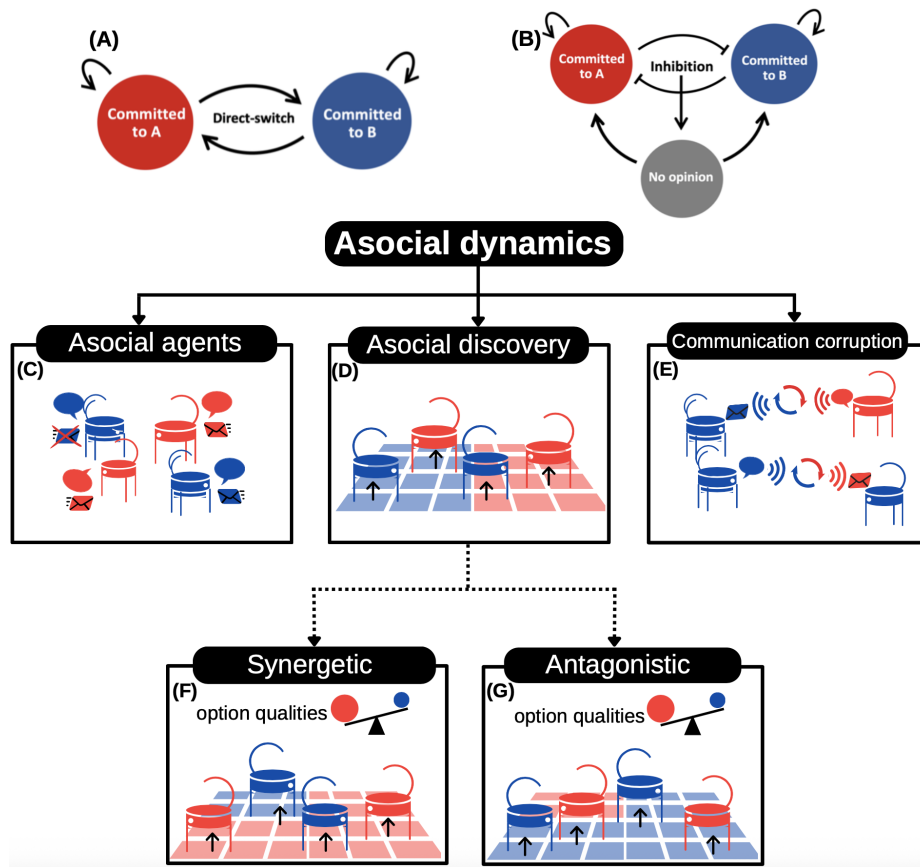


Figure 1. (A-B) The two opinion update mechanisms, direct-switch and cross-inhibition, that the robots use to process social information. With direct-switch (A), robots immediately change their commitment to the received opinion. In cross-inhibition (B), when a committed robot receives a message from a robot with a different opinion, it resets its commitment (it gets inhibited). Only uncommitted robots with no opinion get recruited to either option. (C-G) We consider three types of asocial dynamics impacting the collective decision-making of robot swarms. (C) Asocial agents: in a system where robots interact with each other by sending (speech balloon) and receiving (inbox mail) messages, the presence of asocial agents, such as stubborn agents (zealots), who disregard neighbours' messages and only share their opinion, can influence the collective outcome, leading to indecisions or consensus for suboptimal options. (D) Asocial discovery: robots can occasionally change their opinion by independently self-sourcing information from the environment (e.g., reading the ground colour in the collective perception scenario⁴³) rather than through social interactions. (E) Communication corruption: when robots are impacted by man-in-the-middle (MITM) attacks, the content of messages exchanged among the robots is modified, resulting in the spread of misinformation. (F-G) Environmental evidence can be biased towards either option: (F) a synergistic bias in favour of the best option or (G) an antagonistic bias in favour of the inferior option. Synergistic or antagonistic bias is not limited to asocial discovery (self-sourcing information from the environment), but can also be present in the other asocial dynamics, i.e., different numbers of asocial agents in favour of each option or biased corrupted communication.

We consider two scenarios. The first one is a collective perception scenario frequently studied in swarm robotics research^{43,58,60}, where the swarm's objective is to determine the predominant colour of the ground. In this case, the option

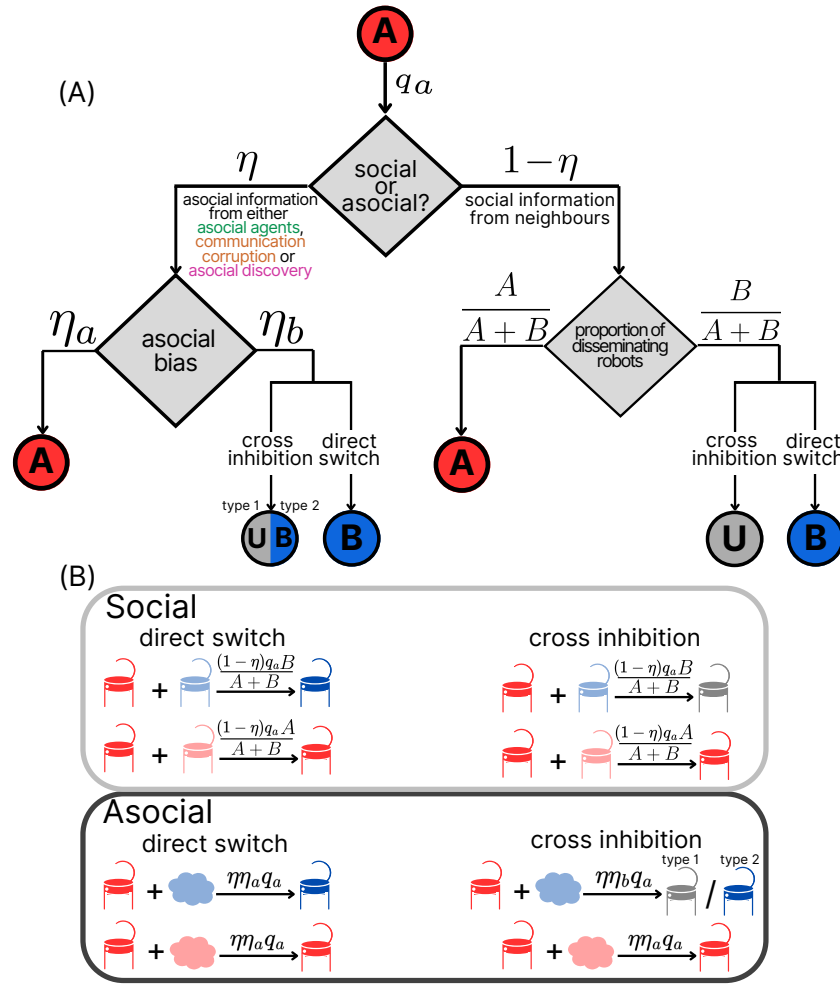


Figure 2. (A) Schematic representation of how a robot supporting option A updates its opinion. The new opinion depends on the information that the robot uses to update its current opinion. The robot either polls ‘representative’ social information with probability $1 - \eta$ or is influenced by asocial dynamics with probability η . When the robot polls representative social information, the probability of reading a message supporting A or B is proportional to the proportion of agents in states A and B, respectively. When influenced by asocial dynamics, such as self-sourcing, asocial agents like zealots, or communication corruption, the information can be biased towards A or B, with weights η_a and η_b , respectively. If the received information (whether social or asocial) is in support of A, the robot retains its opinion regardless of the opinion-update model; if the information supports B, the transition depends on the model: in the cross-inhibition model, the robot becomes uncommitted (U), while in the direct-switch model, it switches to B. In the cross-inhibition model, type 1 asocial dynamics refer to the case where robots become uncommitted (U) when the asocial opinion conflicts with their current opinion, while type 2 is the case where robots directly switch to the asocial opinion (e.g., on self-sourced information). (B) The collective decision-making process presented in (A) can also be described as a chemical reaction network, where transitions happen at rates indicated on top of each arrow. The change of state is triggered by the encounter with another social robot (robots with lighter colours in the top box) or an asocial event (coloured clouds in the bottom box).

qualities q_a and q_b correspond to the proportion of tiles of each colour. This setup leads to synergistic asocial dynamics, where the probability of self-sourcing an option is equal to their quality ($\eta_a = q_a$ and $\eta_b = q_b$); therefore, a higher proportion of red tiles implies both that $q_a > q_b$ and $\eta_a > \eta_b$. To investigate both synergistic and antagonistic biases, we consider a second scenario where we decouple option quality from tile distribution. Here, self-sourcing bias η_a is determined by tile colour proportions, but q_a and q_b are independent quantities reflecting the intrinsic quality of each option as perceived by robots during exploration. This allows us to study antagonistic bias ($\eta_a < 0.5$), where the inferior option is more frequently self-sourced due to greater environmental availability (e.g., more blue tiles despite red being higher quality).

Multiscale modelling: from macroscopic population dynamics to robot swarm simulations

We model the collective decision-making process at multiple levels of abstraction, by combining mechanistic descriptions, deterministic mean-field models, and stochastic simulations. The basic interaction rules are illustrated in Figures 1A-B and 2. Building on these rules, we develop mathematical models by using tools from statistical mechanics⁶⁴ and dynamical systems to describe how the fractions of the population committed to options A and B evolve over time.

Equations (1) and (2)-(3) define the basic ODE models of direct-switch and cross-inhibition, respectively. These models capture the essential dynamics while abstracting from implementation-specific details (as in Figure 2). In contrast, more detailed ODE models can be obtained, such as the robot-specific models presented in the Supplementary Material (Equations SE1 and SE2). These latter models incorporate aspects tailored to the robotic implementation by including the alternating phases of environmental exploration (for quality estimation) and dissemination (for opinion broadcasting). To better understand the system dynamics and, in particular, the underlying stochastic component inherent in the robot experiments, we also formulate the corresponding master equations to account for the stochasticity of finite-sized swarms, in contrast to the deterministic ODE models, which assume an infinitely large population.

Both mean-field models describe the macroscopic dynamics of the system by capturing the time evolution of the fractions of robots committed to option A or B. We analyse these models through equilibrium and stability analysis of the ODEs, where the stable equilibria indicate the long-term collective behaviour of the swarm for $t \rightarrow \infty$. Figure 4 presents a bifurcation diagram showing how the stable and unstable equilibria vary with the frequency of asocial dynamics (η). The diagram shows both basic and robot-specific ODE equilibria (dotted and solid lines, respectively), overlaid with the final state of robot simulations shown as a red 2D histogram. While the basic ODEs capture the robot swarm behaviour only qualitatively, the robot-specific models show close quantitative agreement with the simulations.

To further validate our models, we compare the stationary probability distribution (SPD) obtained from the master equations with the final state of robot simulations (Figure 5 and Supplementary Figure 3). The SPD, computed using the Gillespie algorithm⁵⁷, captures the long-run probability distribution over all possible proportions of the swarm committed to options A and B. We find good agreement among the SPD, the robot simulation results, and the ODE model equilibria, demonstrating the consistency and robustness of our multiscale modelling framework.

Fast, cohesive, accurate, and scalable collective decisions

We systematically compare the performance of the direct-switch and cross-inhibition mechanisms across four dimensions: group cohesion, decision accuracy, decision speed, and scalability.

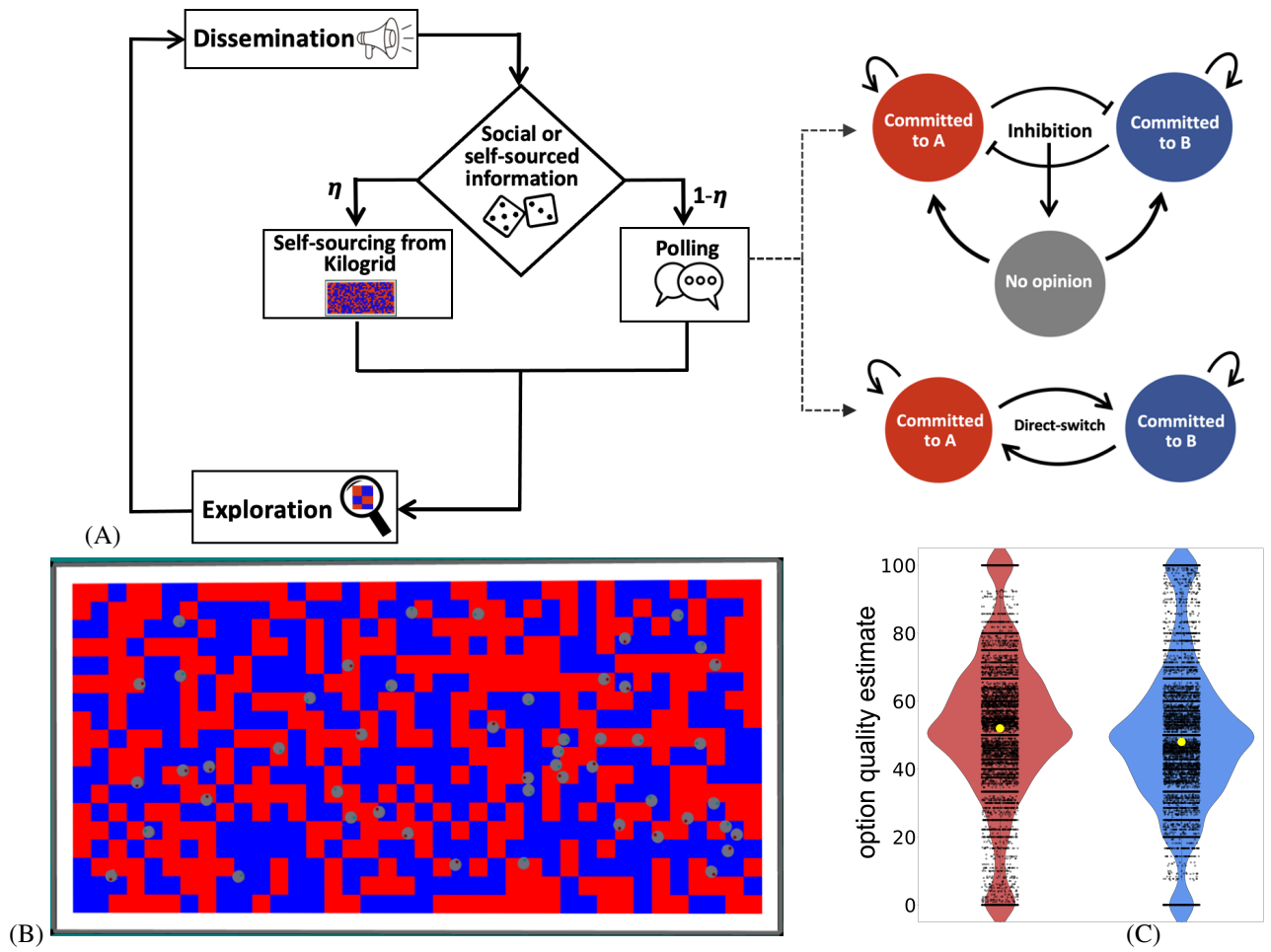


Figure 3. (A) The finite state machine (FSM) describing the robots behaviour, based on the FSM of Valentini et al.²⁰ and extended to include the possibility of asocial dynamics which, in this study, corresponds to self-sourcing information⁴³. The rectangles represent the four FSM states and the arrows represent the transitions among them. The robot updates its opinion based on either social information (polling) or self-sourced environmental information after the dissemination state and moves again to the exploration state after the opinion update. The robots use either direct-switch or cross-inhibition to process social information and update their opinion during polling. (B) Top-view snapshot of an experiment with 50 simulated Kilobots⁶¹ (grey circles) in the Kilogrid^{62,63} arena comprising red and blue tiles. (C) Strip plots overlaid on violin plots showing 7 500 individual quality estimates made by simulated robots for options A (red) and B (blue). The yellow dots on the plot denote the ground-truth proportion of red and blue tiles in the Kilogrid environment.

Cohesion and symmetry breaking

A critical metric of collective decision-making is cohesion, which quantifies the extent of agreement within the swarm as the proportion of agents committed to the majority opinion. Stability analysis of the ODE models (Equations (1) and (2)-(3)) reveals that direct-switch dynamics always yield a single stable equilibrium (Supplementary Text 3). This equilibrium shifts toward either option depending on the interplay between asocial dynamics η , the quality ratio $q = q_a/q_b$, and asocial bias η_a .

Even for relatively low η , asocial bias η_a can offset quality differences (ratio q) and cause decision deadlocks or weak

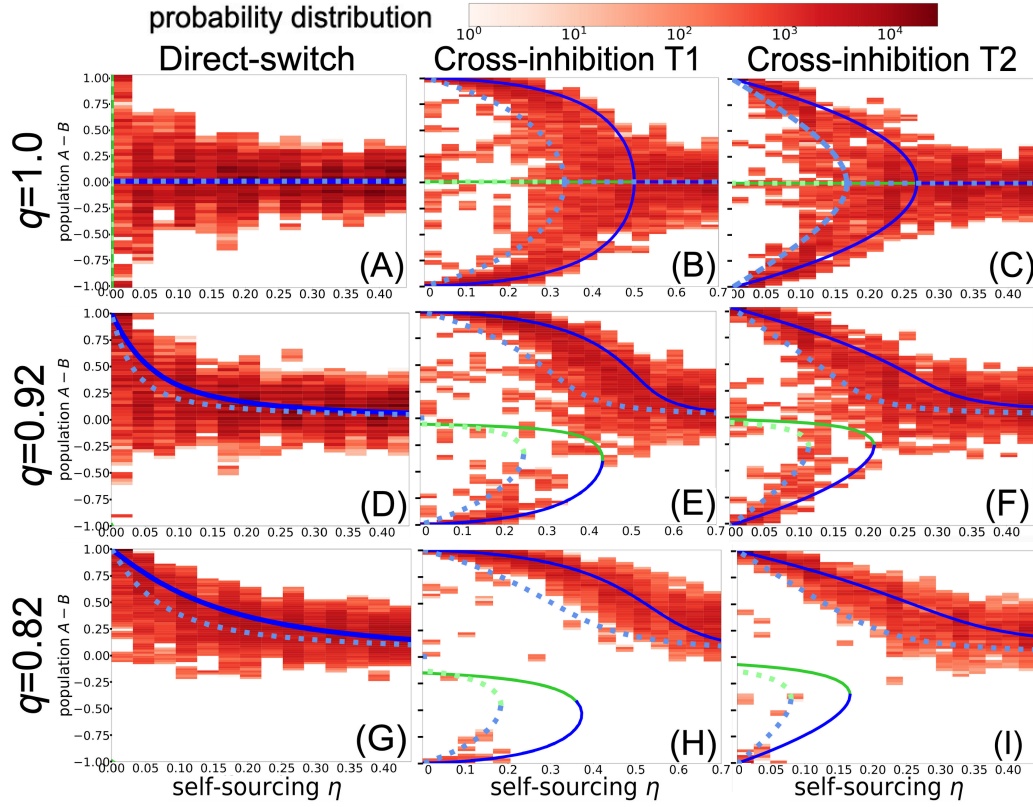


Figure 4. Results from swarm robotics simulations and ODE models. Difference of the proportions of robots $A - B$ (y-axis) as a function of asocial dynamics η (x-axis) for quality ratios $q \in \{1, 0.92, 0.82\}$ (different rows), for direct-switch and cross-inhibition models (different columns), in the collective perception scenario with synergistic bias $\eta_a = q_a$, where quality and self-sourcing are both biased towards the most abundant tile colour⁴³. Cross-inhibition types T1 and T2 correspond to the cases illustrated in Figure 2. 2D histograms (in red) are computed using the last 1000 timesteps (i.e., 6 s) of each of the 50 robot simulation runs per η and subtracting the proportion of robots supporting option B from the proportion of supporters for A , i.e., $(\text{number robots for } A - \text{number robots for } B) / N$. The superimposed lines represent the fixed points of the ODE systems (green are unstable, blue are stable), both of the basic models of Equations (1) and (2)-(3) (dashed lines) and the robot-specific models of Equations SE1 and SE2 (solid lines). The basic ODE model is initialised with agents equally distributed between states A and B , while the robot-specific ODE model is initialised with $t_d/(t_e + t_d)$ agents in dissemination states (split between A_D and B_D), and the rest equally in A_E and B_E . In the robot-specific ODE model and simulations, $t_e = 3000$, $t_u = 1000$ and $t_d = 1300$ (see Methods). Although different, the basic and robot-specific models have qualitatively the same dynamics, which are accurate predictions of the robot simulation results (especially for the latter models). When the two options are of similar (D) or identical qualities (A), the direct-switch approach rarely reaches a stable majority, even with minimal noise. However, with cross-inhibition, regardless of whether the quality differences are small (B,C,E,F) or large (H,I), the population makes a cohesive decision in spite of high asocial dynamics η .

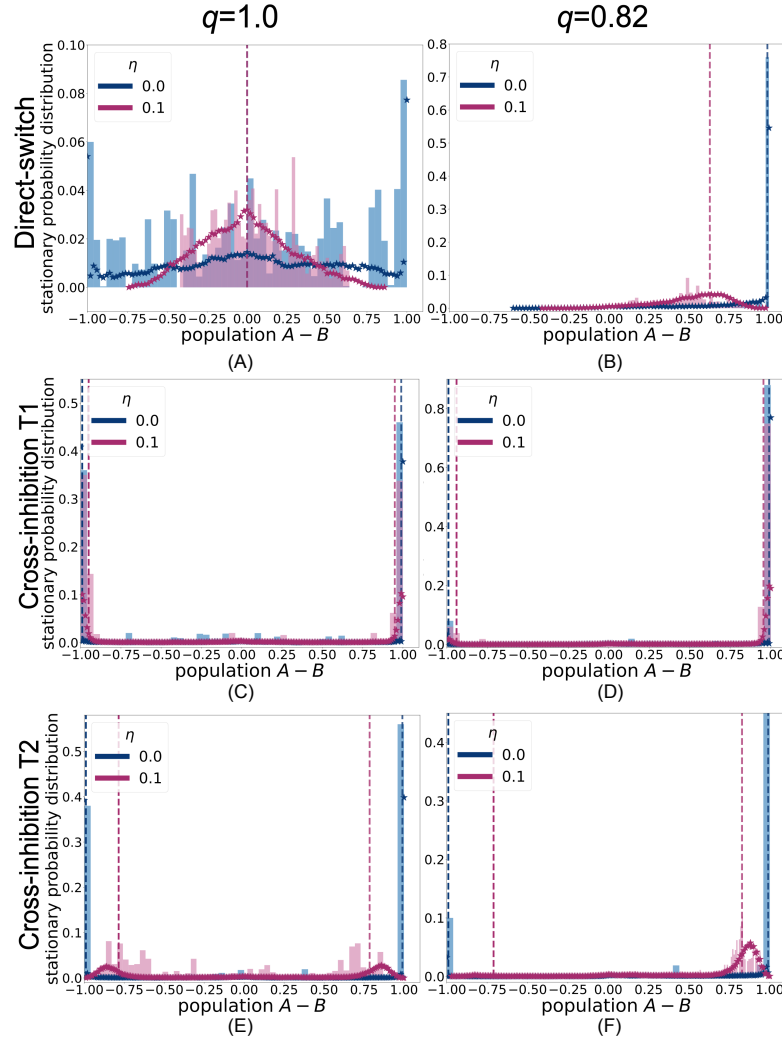


Figure 5. Stationary probability distributions (SPDs) of $N = 100$ robots for $\eta = 0$ (no asocial dynamics) and $\eta = 0.1$ (moderate asocial dynamics), computed using Gillespie's stochastic simulation algorithm (star markers) and robot simulations (histograms). Stable equilibria (from ODE systems of Equations SE1 and SE2) are overlaid as dashed vertical lines. The final distribution of robots (at stability) supporting A and B is consistent across the three analysis methods for two different η values. Each of the 50 Gillespie simulation runs per condition begins with a random initial condition and records the time spent in each state during 200 000 timesteps. The time spent in each state is normalised by the total simulation length to approximate the SPD. The histograms denoting the SPD from robot simulations are computed as the difference between the proportions A and B of robots supporting options A and B, respectively, for each of the last 1 000 timesteps of each of the 50 runs ($(A - B)/N$ on the x-axis). The direct-switch mechanism cannot break the symmetry for low and moderate noise when qualities are symmetric (A), but it never selects the inferior option (B) when qualities are asymmetric. Instead, the cross-inhibition mechanism can always break the symmetry (C,E) but occasionally selects the inferior option (D,F). The probability of choosing the inferior option diminishes in the presence of asocial dynamics ($\eta = 0$ vs $\eta = 0.1$ in D,F).

majorities. The critical bias η_a^* (black line in Figure 6) marks the point at which the majority opinion shifts between options (computed in the Supplementary Text 4). Around this threshold, the system has poor cohesion (light colours in Figure 6).

Cross-inhibition, by contrast, admits multiple equilibria that we study through the bifurcation diagrams of Figures 4 and 7. Direct switch reaches a stable majority for the optimal option only if option qualities differ, i.e., $q \neq 1$ and asocial dynamics are rare (Figure 4D when $\eta \leq 0.05$ or Figure 4G when $\eta \leq 0.1$); otherwise, the swarm remains in an indecisive state, with a similar number of robots committed to either option. On the other hand, cross-inhibition maintains high cohesion across a wide range of parameters, consistent with previous findings^{39,43}. Even under strong asocial dynamics ($\eta \lesssim 0.4$ for noise type-1 and $\eta \lesssim 0.17$ for noise type-2), cross-inhibition breaks symmetry and drives the swarm toward a clear majority, regardless of q or η_a . The marked contrast to the indecision often seen with direct-switch is clearly visible in the cohesion heatmaps of Figure 8A.

Accuracy

Figure 8A also compares the two mechanisms in terms of accuracy, defined as the probability of reaching a large majority where at least $Q = 0.75$ of the swarm selects the best option within $T = 2 \times 10^5$ timesteps. While both mechanisms can fail under extreme asocial biases, their failure modes differ.

Cross-inhibition is cohesive but may settle on the inferior option due to its bistable nature. This can occur when the swarm enters the basin of attraction for the suboptimal equilibrium, driven by initial conditions or stochastic fluctuations (see Supplementary Figure 5). In contrast, direct-switch generally avoids selecting the worse option when the quality difference is moderate ($q = 0.92$ and $q = 0.82$) and asocial dynamics are weak ($\eta < 0.15$). However, under those same conditions, cohesion is low, and decisions are delayed. In fact, the observed accuracy does not result from stable consensus but from transient fluctuations: the system hovers near an indecisive equilibrium, where small majority shifts occasionally cross the quorum threshold Q (see robot distribution in Figures 4, 7). Because the equilibrium is biased toward the better option, these momentary majorities occur more frequently in its favour, yet the system remains attracted to the indecisive state, and decision timing is highly variable (see Supplementary Figure 4).

Notably, moderate levels of asocial dynamics can improve the accuracy of cross-inhibition by eliminating the suboptimal attractor, as previously observed^{37,43}. This effect is evident in the robot results (red histograms) in Figure 4, where the lower suboptimal branch vanishes as η increases, improving decision accuracy (see also Figure 5D,F). Importantly, this improvement is not merely a result of added noise (system temperature to escape the local minima) but asocial dynamics fundamentally alter the system's stability landscape. The bifurcation point η^* marks the transition from bistability to monostability. At this critical point, the swarm achieves maximal accuracy by reliably selecting the better option; however, further increase of η reduces group cohesion. Therefore, zealots, MITM attacks, or independent self-sourcing can equivalently improve decision accuracy by eliminating the possibility of selecting inferior options.

Speed

Cross-inhibition consistently outperforms direct-switch in decision speed, both in selecting any option and in selecting the better one (Figures 8A and Supplementary Figure 4). This speed advantage holds especially under antagonistic bias and is robust to variations in the uncommitted duration t_u (Supplementary Figure 6). Combined speed-accuracy plots computed from robot simulations (Figure 8B-C) further confirm that cross-inhibition is generally faster and more accurate than direct-switch.

Scalability

Beyond asocial dynamics, swarm size N also influences collective decision outcomes⁶⁵. Consistent with prior findings on direct-switch²¹, we observe that larger swarms using cross-inhibition are more accurate (Figures 9A–B). This is due to reduced stochastic fluctuations at larger N ⁶⁴, which make it less likely for the swarm to settle on the suboptimal attractor when starting from two equally-sized subpopulations A and B (see trajectories in Figure 9's insets).

Interestingly, decision speed under cross-inhibition remains nearly constant across swarm sizes (Figures 9C–G), while direct-switch becomes slower as N increases.

Comparison summary

In summary, both direct-switch and cross-inhibition dynamics can be influenced by asocial dynamics η and asocial bias η_a . When the goal is to make quick consensus decisions of the best option, cross-inhibition shows better performance. Cross-inhibition is generally faster, more cohesive, more scalable, and more accurate than (or as accurate as) direct-switch. Only in the absence of asocial dynamics, direct-switch is more accurate than cross-inhibition in selecting between similar quality options but, as soon as asocial dynamics are present, it becomes less cohesive.

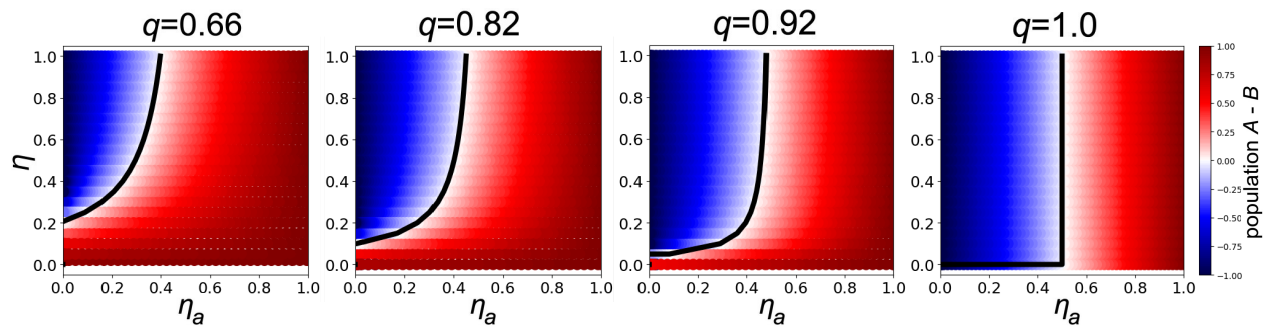


Figure 6. The gradient in the colourmaps shows the long-term population difference between the two options A and B , calculated from the equilibrium of the direct-switch ODE system of Supplementary Equations SE1 as (number of robots in state A - number of robots in state B) / N . Convergence towards option A is represented by red, while blue signifies convergence towards the inferior option B . The black line shows the point of maximum deadlock η_a^* where population of robots for option A equals that for option B . This line is computed in Supplementary Equation 4 as a non-linear function of η (y-axis), η_a (x-axis), and q (values on the top).

Discussion

Minimal mechanisms of social agreement allow groups of simple agents to compensate for individual errors and collectively make fast, accurate, and cohesive decisions. Our analysis reveals that the decision performance can be dramatically altered by the presence of asocial dynamics, which systematically bias the flow of social information. Despite, or thanks to, its simplicity, the biologically grounded mechanism—cross-inhibition—exhibits remarkable robustness.

Previous studies have analysed the dynamics of such mechanisms either under idealised, bias-free conditions^{20,21} or with biases specific to the application scenario^{22,36,43,51}. Our mathematical models unify a broad class of asocial dynamics by

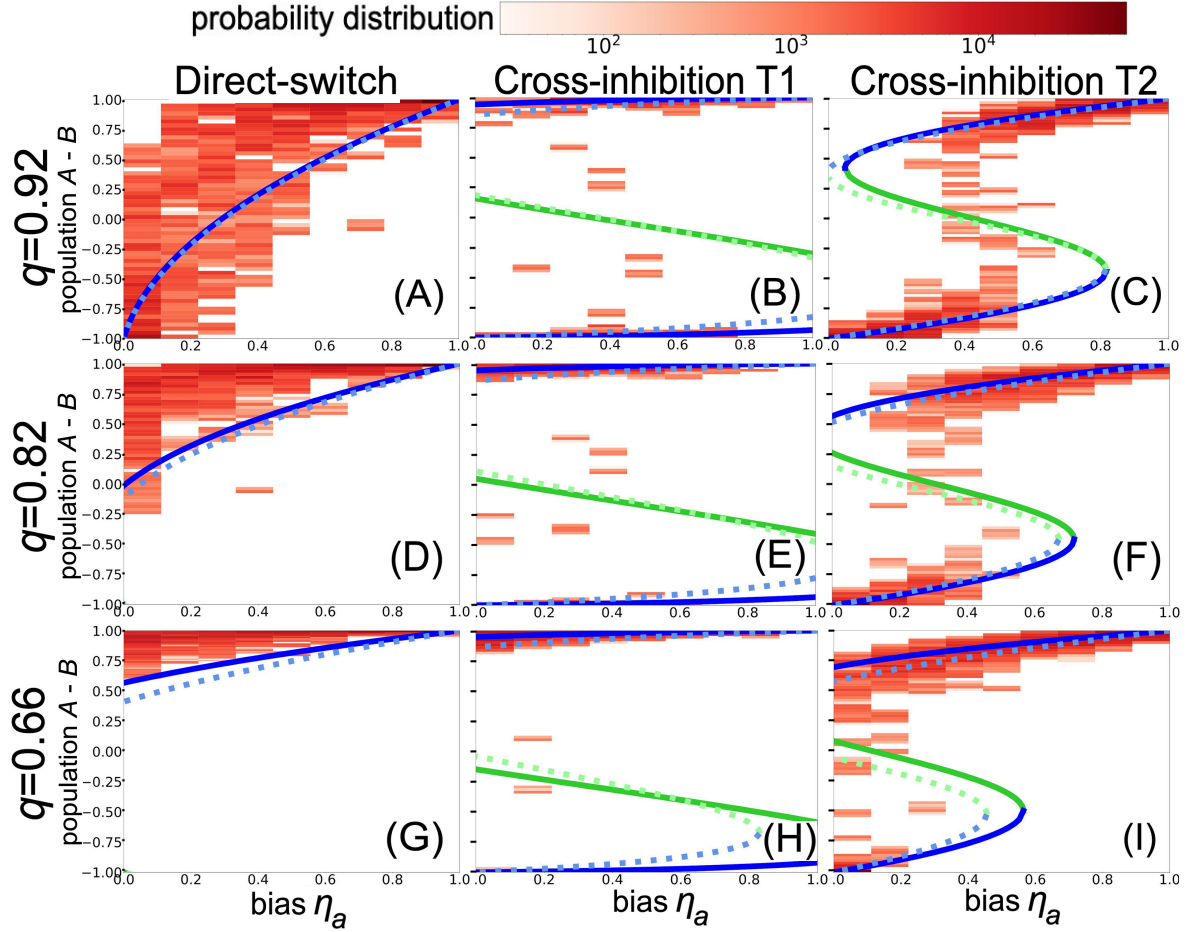


Figure 7. Robot simulation results and ODE bifurcation plot computed in the same way as in Figure 4 using the same parameters unless stated otherwise. Here, we show the difference in the subpopulation sizes $A - B$ as a function of self-sourcing bias for option A (antagonistic bias for $\eta_a < 0.5$, synergistic bias for $\eta_a > 0.5$, and unbiased asocial dynamics for $\eta_a = 0.5$) when $\eta = 0.05$. When the two options are moderately similar (A,D), direct-switch establishes a majority only for a certain range of bias η_a . In (A), $q = 0.92$, for bias values of approximately $\eta_a \approx 0.25$, the two subpopulations are equally sized ($A - B \approx 0$). When quality differences are large (low q) or bias toward the best option is strong (high η_a), direct-switch leads to a majority for the best option, that in certain condition can be relatively slim (e.g., high antagonistic bias $\eta_a \ll 0.5$ in D and G). Instead, cross-inhibition never goes into a state of deadlock and always breaks the symmetry, for any η_a , but can occasionally select the inferior quality option.

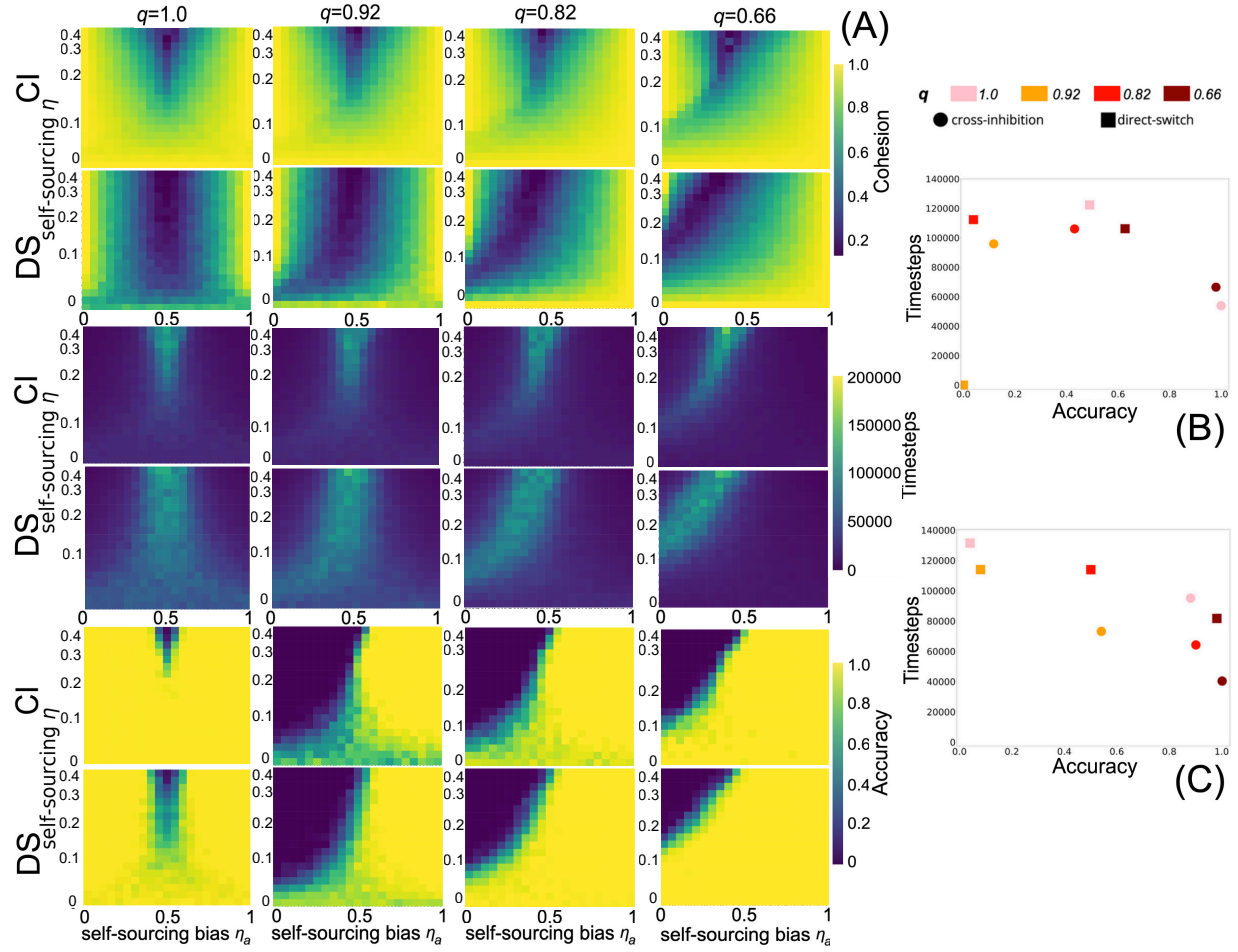


Figure 8. (A) Comparison of the direct-switch and cross-inhibition mechanisms in terms of decision cohesion, speed, and accuracy for increasing asocial dynamics η (y-axis) and increasing asocial bias towards option A, η_a (x-axis). $\eta_a > 0.5$ denotes the case with synergistic bias and $\eta_a < 0.5$ signifies antagonistic case biased towards the lower quality option B. The heatmaps were generated from 100 Gillespie simulations of $T = 200000$ timesteps. Parameters t_d , t_e , and t_u have the same value used with the ODEs analysis and robot experiments presented in Section *Robot experiments*. The results are based on a swarm of $N = 100$ agents with an initial condition of $A_D, B_D, A_E, B_E = [14, 14, 36, 36]$ and for different quality differences $q = \{1, 0.92, 0.82, 0.66\}$. The first two rows compare the two mechanisms in terms of group cohesion; groups using cross-inhibition are more cohesive. The second two rows compare the decision speed, showing that across the parameter space cross-inhibition is quicker than direct-switch. The speed's standard deviation is shown in Supplementary Figure 7. The third two rows compare decision accuracy. Direct-switch shows higher accuracy in the bottom-left region, however this region is also associated to relatively low cohesion. (B-C) The speed vs. accuracy plots generated from the robot simulations show the timesteps to reach consensus (y-axis) and accuracy (x-axis) of the cross-inhibition type 2 (circles) and direct-switch (squares). In (B), $\eta = 0.05$ and $\eta_a = 0.1$, whereas in (C), $\eta = 0.04$ and $\eta_a = 0.5$ for various q . For each configuration, we run 50 robot simulations. The robot results are in agreement with the heatmaps from Gillespie simulations in panel (A).

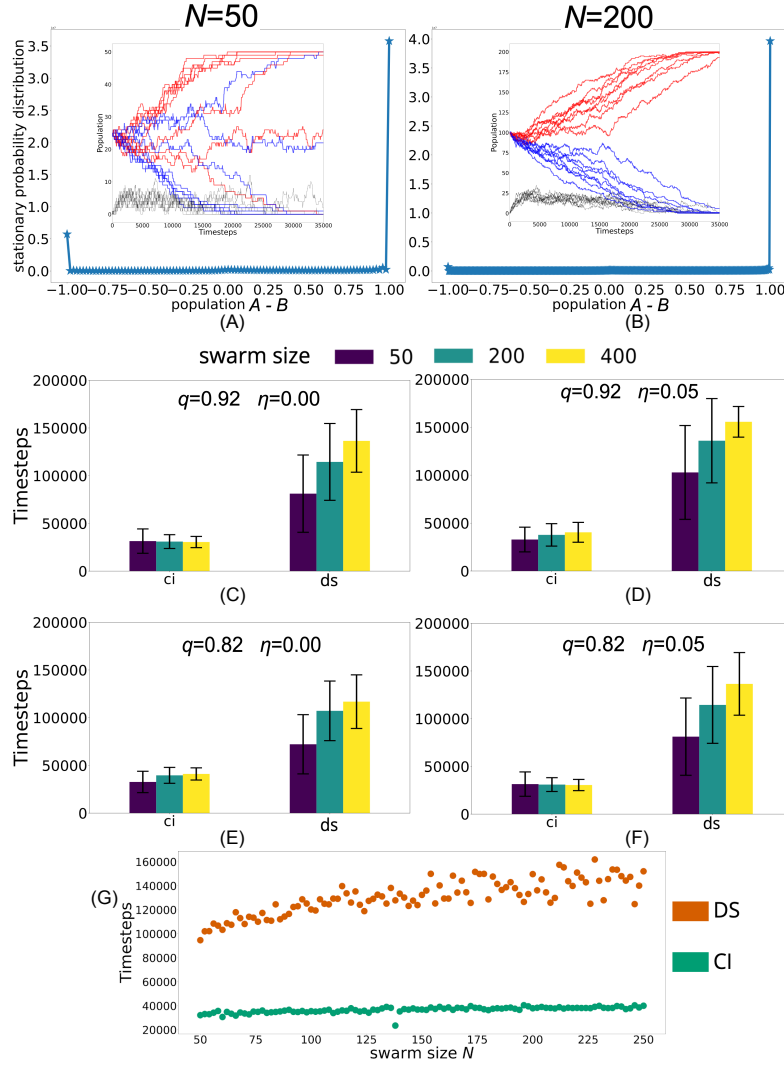


Figure 9. Effect of the swarm size N on decision accuracy (A-B) and decision speed (C-F). Results from 250 Gillespie simulations. (A-B) Stationary probability distribution for cross-inhibition (type-1) for $N = 50$ (A) and $N = 200$ (B), when $q = 0.82$, $\eta = 0$, and the initial distribution of agents between options A and B is equal, i.e., $\{U, A_D, B_D, A_E, B_E\} = [0, 0.14N, 0.14N, 0.36N, 0.36N]$. The insets display the trajectories of 8 of the Gillespie simulation runs used to generate the SPD. The agents utilising cross-inhibition choose the inferior quality option less frequently in large swarms due to reduced stochastic fluctuations. (C-F) Timesteps to make a collective decision (i.e., reach the quorum $Q = 0.7$) for either option for both mechanisms, ci (cross-inhibition type-1) and ds (direct-switch) across three different $N \in \{50, 200, 400\}$ for $q \in \{0.92, 0.82\}$ and $\eta \in \{0, 0.05\}$. (G) Scalability analysis for swarm size $N \in [50, 250]$ for both cross-inhibition (type-1) and direct-switch. Cross-inhibition is faster than direct-switch to converge regardless of swarm size. This scalability analysis excludes physical interference, which can hinder decision-making at high robot densities⁶⁶. We omit this aspect due to its strong dependence on specific robots, environments, and context-specific mitigation strategies.

representing them through equivalent terms in the opinion update equations, enabling systematic and exhaustive analysis of their effects on collective decision-making. Equivalent biased dynamics arise when swarms (i) include a proportion of stubborn individuals (zealots) who share a fixed opinion and never update it^{38,39,42}, (ii) experience miscommunication due to, for instance, man-in-the-middle (MITM) attacks that alter message content^{37,56}, or (iii) comprise individuals who occasionally self-source information from the environment^{27,51}. Self-sourcing can be necessary for adaptation to environmental changes^{22,67}, while the presence of zealots or corrupted communication may be unavoidable due to faults or cyberattacks^{41,42,47}. These challenges are not unique to artificial systems. Natural systems must also resolve internal conflicts, as in animal groups with informed individuals pursuing opposing goals^{53,54}, or human collectives where misinformation can shape decision outcomes^{52,68}.

While direct-switch is typically more accurate than cross-inhibition in the absence of asocial dynamics (Figure 5), our analysis shows that even mild asocial influence often drives the swarm into a state of decision deadlock. Cross-inhibition, a biologically inspired mechanism qualitatively equivalent to decision-making models in house-hunting honeybees⁵ and neural circuits^{14,16,69}, enables faster, more cohesive, and more accurate decisions under a wide range of biased conditions. Despite strong asocial dynamics, robot swarms using cross-inhibition consistently outperformed those using direct-switch. Our results reveal a previously unrecognised robustness and scalability of cross-inhibition, which may explain its recurrence across biological systems.

Cross-inhibition has been linked to better management of the speed-value trade-off^{25,70}, where decision value reflects the reward obtained from the selected option. By enabling consensus even among similar options or under strong bias, cross-inhibition can occasionally lead to the selection of a suboptimal alternative. Natural systems such as brains and insect colonies may favour coherence and speed over accuracy, preferring a rapid, unified choice over prolonged indecision¹⁶. For example, honeybees may have evolved the stop signal to prevent swarm splitting during nest-site selection^{5,27}. In contrast, ants lack such inhibitory signalling⁷¹, possibly because split colonies can reunite days after relocation³⁴. Inhibitory signalling between competing integrators of noisy evidence also enables winner-take-all dynamics in other domains, from mitotic checkpoint control^{28,29} to neural decision-making via leaky competing accumulator models^{14,16}. The recurrence of cross-inhibition across such diverse systems suggests it may be a particularly robust and scalable solution for fast, cohesive decision-making.

Our analysis reveals that cross-inhibition is not only robust to asocial biases but can also be antifragile to them. Antifragility⁷² refers to the property of systems that improve when exposed to moderate stressors. In collective decision-making, this is exemplified by systems that perform better under moderate levels of miscommunication^{37,67} or balanced groups of stubborn agents (zealots)^{36,48}. Our bifurcation analysis shows that the performance gains from asocial dynamics are not solely attributable to increased randomness (system temperature) but also to structural changes in the system's phase space. Performance peaks near the edge of criticality, where the system balances flexibility and stability—a regime that has also been shown to enhance responsiveness and adaptability in other collective systems requiring agile behaviour^{73,74}. Since asocial dynamics may be inherent in natural or engineered systems, mechanisms that benefit from such disturbances—rather than merely resist them—offer a powerful design paradigm. Cross-inhibition, identified through biological inspiration, exemplifies this potential.

Our analysis clarifies the trade-offs of robot swarms running algorithms based on either mechanism. Under asocial dynamics, direct-switch and cross-inhibition reveal distinct vulnerabilities analogous to denial-of-service (DoS) and wrong-addressing attacks—concepts borrowed from cybersecurity. DoS, where a system is overwhelmed and rendered unresponsive, mirrors how direct-switch can become locked in indecision under antagonistic bias. Conversely, wrong-addressing, akin to astroturfing

that skews perception toward a misleading outcome, parallels cross-inhibition's tendency to select a suboptimal option when qualities are similar. These analogies highlight distinct failure modes and help characterise the specific risks associated with each decision-making mechanism.

Certain application scenarios may benefit from the dynamics of direct-switch. When robot opinions are reported to human operators, prolonged indecision or slim majorities can serve as valuable indicators of ambiguous or difficult choices between similarly valued options. In certain cases, delaying action may even be advantageous, allowing the system to remain inactive until clearer information emerges or until acting becomes safe.

By contrast, cross-inhibition is more suitable for autonomous swarm systems that must act decisively without human intervention. It enables rapid consensus even when option qualities are close, favouring operational responsiveness over guaranteed optimality. This makes it well-suited for tasks where timely action is critical, for example, swarms tasked with identifying the agricultural field most in need of treatment⁷⁵, selecting the first chemical spill to contain, or prioritising the most urgent firefighting front¹¹.

We investigated two key decision-making mechanisms in their minimal form. While combining social and asocial information is optimal in several biological collectives^{76,77}, the relative weighting of these sources critically shapes the group dynamics^{27,67}. We envision future algorithms in which robots dynamically adjust the balance between social and asocial inputs to steer the system toward criticality, conditions that, as our analysis suggests, enhance collective decision-making performance. A key challenge lies in the limited information available to individual agents, who must rely on local cues to adjust their behaviour, for example, using proximate indicators such as estimated local consensus⁶, interaction frequency⁷⁸, or urgency of action³³. Future strategies might also hybridise direct-switch and cross-inhibition—e.g., incorporating periodic opinion resets to escape local minima⁷³—or address more complex asocial behaviours, such as contrarians with population-dependent biases^{37,47}. Finally, the structure of the interaction network plays a key role in shaping group decision-making^{35,77}: dynamically adjusting network topology could give individuals additional leverage to steer collective dynamics or mitigate asocial biases²².

Methods

Mean-field models of the basic collective decision-making algorithm

The opinion dynamics of the swarm can be modelled by using mean-field models, in the form of a system of ordinary differential equations (ODEs). This model assumes the continuous limit $N \rightarrow \infty$, that is, the swarm has infinite size (finite-sized system models are discussed in the Section *Stochastic Analysis*). This assumption is effective for making good approximations of large-scale, well-mixed systems and enables the use of dynamical systems and bifurcation analysis to generate deterministic predictions of the system's behaviour^{73,79}.

We focus on the best-of- n decision problem with $n = 2$ options, where a swarm of N agents—or robots—exchange information in order to select collectively the best option. Options A and B are associated with a quality value, q_a and q_b , respectively. The ratio of the two qualities is $q = q_b/q_a$. Without loss of generality, we assume that $q_a \geq q_b > 0$, which implies that $q \in (0, 1]$. How an agent committed to A (in state A), committed to B (in state B), or uncommitted (state U) changes its opinion depends on the opinion update mechanism. We consider two mechanisms: direct-switch and cross-inhibition (see Figure 1A-B).

Let a, b , and u be the proportions of robots in the states A, B, and U, respectively. Note that, in this basic models, we do not

consider separated dissemination and exploration phases (which are only relevant to the robot-specific model, presented in the Supplementary Equation SE1).

The ODE system for the direct-switch model with generic asocial dynamics reads as

$$\frac{da}{dt} = ab(1 - \eta)(q_a - q_b) + \eta(b\eta_a - a\eta_b) \quad (1)$$

where $b = 1 - a$.

The ODE system for the cross-inhibition model with generic asocial dynamics reads as

$$\frac{da}{dt} = a(1 - \eta)(q_a u - q_b b) + \eta(u\eta_a - a\eta_b) \quad (2)$$

$$\frac{db}{dt} = b(1 - \eta)(q_b u - q_a a) + \eta(u\eta_b - b\eta_a) \quad (3)$$

where $u = 1 - a - b$.

In the direct-switch model, the proportions a and b increase or decrease when a robot in state A (or B) directly switches to B (or A) after interacting with a robot committed to the opposite opinion, namely following a social interaction occurring with probability $1 - \eta$. This interaction occurs with a frequency proportional to the quality of the option held by the neighbour, i.e., q_a or q_b . The proportions of robots a and b also change due to asocial dynamics occurring at rate η . A robot in state A (or B) switches to B (or A) at a rate $\eta\eta_b$ (or $\eta\eta_a$).

Similarly, in cross-inhibition, an uncommitted robot U gets recruited to option A or B after interacting with a committed robot, also happening at a rate proportional to q_a or q_b , respectively; once again, this social interaction occurs with probability $1 - \eta$. Proportions a and b also decrease at rates $(1 - \eta)q_b$ and $(1 - \eta)q_a$, respectively, when interaction among robots committed to different options occurs. An uncommitted robot—in state U —switches to A (or B) at a rate $\eta\eta_a$ (or $\eta\eta_b$), and committed robots in state A (or B) become uncommitted at rate $\eta\eta_b$ (or $\eta\eta_a$). When $\eta_a > \eta_b$, asocial dynamics are synergistic, while when $\eta_a < \eta_b$, they are antagonistic.

Collective perception through robot-specific collective decision-making algorithms

The basic algorithms modelled in the previous section can be instantiated to make best-of- n (best-of-2 in our case) decisions in a robot swarm. Robots are physical devices that need to operate under the technical constraints of the platform, requiring them to sense and sample the environment to determine the quality of options. Therefore, we extend the basic decision-making algorithms by including two alternating phases: exploration and dissemination.

The robot behaviour can be described by the finite state machine shown in Figure 3A. Agents can be distinguished into five possible states: A_D (disseminating opinion A), B_D (disseminating opinion B), A_E (exploring option A), B_E (exploring option B) and U (uncommitted to any option). Robots in the exploration phase sample the environment and estimate the quality of their current opinion (i.e., option A or B). The duration of the exploration state (t_e) for a robot is determined by a random draw from an exponential distribution with a rate of $\lambda_e = t_e^{-1}$. Therefore, robots leave the exploration state after a mean time t_e and transition to the dissemination phase (state A_D or B_D). Robots in the dissemination state share their opinions (i.e., option A or B) locally with their neighbouring robots. The duration of time a robot disseminates its opinion is determined by a random draw from an exponential distribution with rate $\lambda_d = (q_i t_d)^{-1}$. Consequently, the average time spent by the robot in the dissemination state is directly proportional to the assessed quality q_i (where $i = \{a, b\}$) of the estimated option, which the robot has assessed

during the exploration phase. Uncommitted robots stay in the uncommitted state U for an average time t_u , during which they do not estimate or disseminate any option.

At the end of the dissemination state or the uncommitted state, the robot updates its opinion through polling social information, i.e., it changes its opinion based on information polled from neighbouring robots. This polling phase can also be affected by asocial dynamics caused by zealots, MITM attacks, or independent self-sourcing of information by the robots (see Supplementary Figure 8). Depending on the type of asocial dynamics, the mechanism is different, leading however to the same probabilistic process. With probability $1 - \eta$, the robot polls ‘representative’ social information from one of its neighbours (i.e., with probabilities biased towards the opinions of the population). With probability η , the robot polls asocial information which can either be broadcast by a zealot robot, be corrupted via an MITM attack, or be independently sourced from the environment by the robot. In the latter case, to be precise, the robot does not undergo polling but spontaneously decides to not use social information and instead updates its opinion by looking at the environment. In this work, we implement our analysis on independently sourced information from the environment.

Depending on the outcome of the polling action (or self-sourcing), the robot returns to an exploration state A_E or B_E , or to the uncommitted state U (see Figures 3 and supplementary Figure 8).

There are **two main differences** between this robot algorithm and the basic one: the decision-making dynamics are slower—due to the additional dissemination state—and only a proportion of committed agents broadcast messages. When the robot, with probability $1 - \eta$, polls the representative social information (right branch in Supplementary 8), it only polls information from the robots in disseminating state, i.e., in states A_D and B_D . Hence, the robot processes a message for option A with probability $A_D/(A_D + B_D)$ and a message for option B with probability $B_D/(A_D + B_D) = 1 - [A_D/(A_D + B_D)]$. These differences lead to a slight change in the dynamics and equilibria but to qualitatively similar results (see Figures 4 and 7). The ODEs modelling the robot experiments are detailed in the Supplementary Text 2.

Stochastic Analysis

In Supplementary Text 2, we modelled the behaviour of the two collective decision-making algorithms by using the continuous limit approximation, where the swarm size N approaches infinity. However, real-world swarm systems are composed of a large yet finite number of agents. The finite number of agents can cause random (size-dependent) fluctuations, which can have a significant impact on the system dynamics^{80,81}. Therefore, it is always important to verify whether the predictions based on continuous approximations hold in the presence of size-dependent fluctuations. To study finite-size effects in a computationally efficient way, we use the formalism of chemical master equations, which are derived from a chemical-like reaction network^{57,64}. Chemical master equations are stochastic differential equations that model molecules undergoing coupled reactions. In a multi-agent system, agent states are represented by molecule types, and state transitions are represented as chemical reactions with specific rates. The transitions for the algorithms based on direct-switch and cross-inhibition mechanisms in our system are specified in the Supplementary Text 6.

The chemical reaction network and relative master equation are advantageous because they allow the study of random fluctuations with a magnitude that is not arbitrarily decided by the modeller but rather based on a principled approach and inversely proportional to system size N ⁶⁴. This means that as the swarm size N increases, the random fluctuations become smaller, and in turn, the predictions of the chemical reaction network converge to those of the noiseless ODE model. Solving

chemical master equations analytically can be challenging or even sometimes unfeasible. Hence, to investigate such systems, we resort to numerical simulations utilising the Gillespie algorithm⁵⁷. Unless stated otherwise, the analyses of models using Gillespie algorithm are based on 50 long Gillespie simulations, lasting 20 000 timesteps each. These simulations use the same transition rates as the ODE models and robot experiments, with each run initialised using random initial conditions where the number of robots in each state is drawn uniformly at random.

Robot experiments

To perform robot experiments, we consider a case study designed after the collective perception scenario outlined in⁴³, where the robots are tasked with selecting the most important element in the environment. In our case, the floor is composed of randomly distributed red and blue tiles (see Figure 3B), and the swarm must collectively select one of the two colours. Therefore, the colours are the two options—A is red, B is blue.

Synergistic and antagonistic environmental biases

The values η_a and η_b indicate the proportion of tiles allocated to each option (red and blue, respectively), which define the probability of discovering that option. When we consider synergistic asocial dynamics, the proportion of tiles in each colour is linearly proportional to the quality of each option, i.e., $\eta_a = q_a/(q_a + q_b)$ and $\eta_b = 1 - \eta_a = q_b/(q_a + q_b)$. More precisely, the abundance of each colour represents its quality^{24,58,60}. Therefore, to estimate the option quality and collectively select the most frequent colour in the environment, robots count the proportion of tiles of each colour.

With antagonistic asocial dynamics, the option quality is inversely proportional to the probability of self-sourcing them. This scenario corresponds to the case where robots discover options with inferior quality more easily than the best option (which is more difficult to find)²⁶. The proportion of tiles of each colour only determines the bias in discovering either option (i.e., robots find the more abundant colour more often). Instead, the quality is not represented by the abundance of each colour but is an independent quantity that robots estimate from the environment.

Simulation setup

We simulate a swarm of $N = 100$ robots modeled after the Kilobot platform⁶¹. The Kilobots are low-cost and small-sized robots that move at a speed of 1 cm/s, rotate in place at 45 °/s, and communicate with each other in a range of 10 cm through infrared (IR), and whose control loop operates at an approximate interval of 32 ms. We utilize a simulation of the Kilogrid system^{62,63}, a customizable and interactive environment specifically tailored for the Kilobots. The Kilogrid, which comprises 800 cells, allows the robots to self-source options via IR communication and assess the quality of their opinions during exploration. In the case of synergistic bias, the proportion of cells of each colour represents both the option quality and the asocial dynamics bias. Therefore, when $q_a = q_b$, 50% tiles are red and 50% tiles are blue, and when $q_a \neq q_b$, the ratio between q_a and q_b defines the proportions of cells of each colour. In our experiments, we test three different proportions of tiles in the Kilogrid: 50%A-50%B ($q = 1$, no quality difference), 52%A-48%B ($q = 0.92$, small quality difference) and 55%A-45%B ($q = 0.82$, moderate quality difference). In the case of antagonistic bias, the quality is a number in the range $q_i \in [0, 1]$ communicated by the Kilogrid. Given a percentage of red and blue cells, their distribution in the Kilogrid is uniformly random. All the cells, except for those at the borders (shown in white in Figure 3B), are programmed to continuously transmit IR messages containing their ID, their colour, and (in the antagonistic case study) the quality value q_i . Both the Kilobots and the Kilogrid are simulated in ARGoS through dedicated plugins^{82,83}.

Initialisation

At the beginning of each run, we initialise the robots in the exploration state with a random initial opinion, with half of the swarm committed to option A (in state A_E), and the other half committed to option B (in state B_E). We deploy the robots on the Kilogrid at uniformly random initial positions. The distribution of Kilogrid tiles is randomly regenerated for each run. Each run lasts $T = 200\,000$ simulation timesteps, equivalent to 110 minutes.

Robot behaviour

To explore different areas of the environment and interact with different robots, the Kilobots perform a random walk in the environment to encounter various robots in their vicinity during the dissemination phase, and to provide a more accurate estimation of the option qualities from the Kilogrid during the exploration phase. Due to the absence of proximity sensors in Kilobots, the Kilogrid cells transmit a binary ‘wall flag’ (either high or low) to signal proximity to a wall. The white cells at the borders and the non-white cells adjacent to them send a high wall flag, while all the other internal cells send a low flag. When a robot receives a high wall flag from the Kilogrid, it executes a basic obstacle avoidance routine regardless of its current state.

The robot behaviour during the exploration phase is different in the synergistic and antagonistic cases. In the synergistic case, a robot committed to an option reads Kilogrid messages to keep track of the number of cells encountered, denoted by T_c , and the number of cells visited that share the same colour as its opinion i , represented by C_i . The robot ensures that each cell is counted only once by using the cell’s ID. At the end of the exploration cycle, the robot estimates the quality, indicated by $q_i = C_i/T_c$. The values T_c and C_i represent the counts obtained during a single exploration cycle and are reset before entering the dissemination state. If the robot never visits a cell corresponding to i , it sets the estimated quality to $q_i = 0$. In the antagonistic case, the robot makes an immediate quality estimate q_i as soon as it visits one cell with the same colour as its opinion i . The quality estimate communicated by the cell is sampled from a normal distribution $\mathcal{N}(q_i, \sigma)$, where q_i is the nominal quality value, either q_a or q_b , and σ is the sampling noise. The σ value is set by computing the standard deviation of the noisy quality estimates the robots obtain from the Kilogrid, relative to the nominal quality values. To keep the two cases as comparable as possible, the average length of the exploration phase is kept the same for both the synergistic and antagonistic cases. Based on q_i , the robot calculates the dissemination time using an exponential distribution with $\lambda_d^{-1} = q_i t_d$, where t_d denotes the average number of control cycles in dissemination when q_i equals 1, and is equal to 1 300 in our setup. This value corresponds to a λ_d^{-1} of approximately 40 seconds. Uncommitted robots move randomly in the environment for an average of $t_u = 1\,000$ control cycles (approximately 30 seconds) without making any quality estimate or sending any message. Then, they move to the polling or self-sourcing phase.

After dissemination, the robot determines with probability η whether to conduct an individual self-sourcing of the environment or engage in social interaction to update its opinion. If the robot chooses to self-source, it switches its opinion to the option (colour) of the cell in its current position. Therefore, the proportions of tiles of each colour η_a and η_b determine the probability of switching opinion to A or B, respectively. In the synergistic case, $\eta_a = q_a/(q_a + q_b)$, hence switching to state A_E , in favour of the higher quality option A, is more probable than switching to B_E . In the antagonistic case, we assume $q_a > q_b$, hence $\eta_a < \eta_b$.

Given our robots have extremely limited memory and computation, during the polling phase a robot only considers the first message it receives from its neighbours, which it uses to update its opinion using either direct-switch or cross-inhibition. Once the environmental self-sourcing or polling phase is complete, the robot calculates the exploration time and returns to

the exploration state. A committed robot calculates the exploration time using $\lambda_e^{-1} = t_e = 3000$, resulting in an average exploration time of approximately 100 seconds. Throughout the paper, the t_d , t_e , and t_u values of the ODE model and the Gillespie simulations in all the analyses are fixed to the values used for robot experiments.

Speed-accuracy and speed-cohesion metrics

We analyse the relationship between decision speed, collective accuracy, and group cohesion using the following metrics.

Cohesion reflects the degree to which the agents, or robots, choose the same option. A run is said to be cohesive if all the robots (i.e., the whole swarm) choose the same option³⁴. We compute cohesion as the size of the largest sub-population at termination time T , obtained by determining the absolute population difference, i.e., $|\text{number robots for A} - \text{number robots for B}| / N$, where $|\cdot|$ is the absolute value operator. For each specific configuration of q , η , and η_a , we report the average cohesion across the set of executed runs.

Accuracy represents the probability that the swarm chooses the best option. For each tested configuration, we compute accuracy by calculating the proportion of runs that reached the quorum $Q = 0.75$ for the best option A. A run is considered accurate when $A_D + A_E \geq N \times Q$, i.e., 75% of the population has selected option A. When the two options are of equal quality (i.e., $q = 1$), reaching quorum Q for either option is considered an accurate decision.

Decision speed measures how quickly the swarm reaches a collective decision. We compute decision speed as the average number of timesteps taken to reach the quorum $Q = 0.75$ in favour of any option. Therefore, runs that fail to reach the quorum within the designated time limit T are disregarded.

References

1. Hamann, H. *Swarm Robotics: A Formal Approach* (Springer Publishing Company, Incorporated, 2018), 1st edn.
2. Carrillo-Zapata, D. *et al.* Mutual shaping in swarm robotics: User studies in fire and rescue, storage organization, and bridge inspection. *Front. Robotics AI* **7**, DOI: [10.3389/frobt.2020.00053](https://doi.org/10.3389/frobt.2020.00053) (2020).
3. Reina, A., Ferrante, E. & Valentini, G. Collective decision-making in living and artificial systems: editorial. *Swarm Intell.* **15**, 1–6, DOI: [10.1007/s11721-021-00195-5](https://doi.org/10.1007/s11721-021-00195-5) (2021).
4. Bonabeau, E., Dorigo, M. & Theraulaz, G. *Swarm Intelligence - From Natural to Artificial Systems* (Oxford University Press, 1999).
5. Seeley, T. D. *et al.* Stop signals provide cross inhibition in collective decision-making by honeybee swarms. *Science* **335**, 108–111, DOI: [10.1126/science.1210361](https://doi.org/10.1126/science.1210361) (2012).
6. March-Pons, D., Múgica, J., Ferrero, E. E. & Miguel, M. C. Honeybee-like collective decision making in a kilobot swarm. *Phys. Rev. Res.* **6**, 033149 (2024).
7. Ballerini, M. *et al.* Empirical investigation of starling flocks: a benchmark study in collective animal behaviour. *Animal Behav.* **76**, 201–215, DOI: [10.1016/j.anbehav.2008.02.004](https://doi.org/10.1016/j.anbehav.2008.02.004) (2008).
8. Ferrante, E. *et al.* Self-organized flocking with a mobile robot swarm: a novel motion control method. *Adapt. Behav.* **20**, 460–477, DOI: [10.1177/1059712312462248](https://doi.org/10.1177/1059712312462248) (2012).

9. Garnier, S., Combe, M., Jost, C. & Theraulaz, G. Do ants need to estimate the geometrical properties of trail bifurcations to find an efficient route? A swarm robotics test bed. *PLoS Comput. Biol.* **9**, 1–12 (2013).
10. Hauert, S. & Bhatia, S. N. Mechanisms of cooperation in cancer nanomedicine: towards systems nanotechnology. *Trends Biotechnol.* **32**, 448–455, DOI: <https://doi.org/10.1016/j.tibtech.2014.06.010> (2014). Special Issue: Next Generation Therapeutics.
11. Tzoumas, G., Salina, L., McConville, A., Richardson, T. & Hauert, S. *Extinguishing Wildfires in Large Scale Scenarios Using Swarms of UAVs*, 71–83 (2024).
12. Valentini, G., Ferrante, E. & Dorigo, M. The best-of-n problem in robot swarms: Formalization, state of the art, and novel perspectives. *Front. Robotics AI* **4**, 9, DOI: [10.3389/frobt.2017.00009](https://doi.org/10.3389/frobt.2017.00009) (2017).
13. Seeley, T. D. & Buhrman, S. C. Nest-site selection in honey bees: how well do swarms implement the "best-of-n" decision rule? *Behav. Ecol. Sociobiol.* **49**, 416–427 (2001).
14. Usher, M. & McClelland, J. L. The time course of perceptual choice: the leaky, competing accumulator model. *Psychol. review* **108**, 550–92, DOI: [10.1037//0033-295X.108.3.550](https://doi.org/10.1037//0033-295X.108.3.550) (2001).
15. Marshall, J. A. R. *et al.* On optimal decision-making in brains and social insect colonies. *J. The Royal Soc. Interface* **6**, 1065–1074, DOI: [10.1098/rsif.2008.0511](https://doi.org/10.1098/rsif.2008.0511) (2009). <https://royalsocietypublishing.org/doi/pdf/10.1098/rsif.2008.0511>.
16. Pirrone, A., Reina, A., Stafford, T., Marshall, J. A. & Gobet, F. Magnitude-sensitivity: rethinking decision-making. *Trends Cogn. Sci.* **26**, 66–80, DOI: [10.1016/j.tics.2021.10.006](https://doi.org/10.1016/j.tics.2021.10.006) (2022).
17. Reina, A., Bose, T., Trianni, V. & Marshall, J. A. R. Psychophysical laws and the superorganism. *Sci. Reports* **8** (2018).
18. Reina, A., Dorigo, M. & Trianni, V. Collective decision making in distributed systems inspired by honeybees behaviour. In Lomuscio, A. & et al. (eds.) *Proceedings of the 13th International Conference on Autonomous Agents and Multiagent Systems*, 1421–1422 (IFAAMAS, Richland, SC, 2014).
19. Hunt, E. R. & Hauert, S. A checklist for safe robot swarms. *Nat. Mach. Intell.* **2**, 420–422, DOI: [10.1038/s42256-020-0213-2](https://doi.org/10.1038/s42256-020-0213-2) (2020).
20. Valentini, G., Hamann, H. & Dorigo, M. Self-organized collective decision making: The weighted voter model. In *Proceedings of the 13th International Conference on Autonomous Agents and Multiagent Systems*, AAMAS '14, 45–52 (IFAAMAS, Richland, SC, 2014).
21. Valentini, G., Ferrante, E., Hamann, H. & Dorigo, M. Collective decision with 100 Kilobots: Speed versus accuracy in binary discrimination problems. *Auton. Agents Multi-Agent Syst.* **30**, 553–580 (2016).
22. Talamali, M. S., Saha, A., Marshall, J. A. R. & Reina, A. When less is more: Robot swarms adapt better to changes with constrained communication. *Sci. Robotics* **6**, eabf1416, DOI: [10.1126/scirobotics.abf1416](https://doi.org/10.1126/scirobotics.abf1416) (2021). <https://www.science.org/doi/pdf/10.1126/scirobotics.abf1416>.
23. Shan, Q. & Mostaghim, S. Discrete collective estimation in swarm robotics with distributed Bayesian belief sharing. *Swarm Intell.* **15**, 377–402 (2021).

24. Bartashevich, P. & Mostaghim, S. Benchmarking collective perception: New task difficulty metrics for collective decision-making. In Moura Oliveira, P., Novais, P. & Reis, L. P. (eds.) *Progress in Artificial Intelligence*, 699–711 (Springer International Publishing, Cham, 2019).
25. Pais, D. *et al.* A mechanism for value-sensitive decision-making. *PLoS ONE* **8**, 1–9, DOI: [10.1371/journal.pone.0073216](https://doi.org/10.1371/journal.pone.0073216) (2013).
26. Reina, A., Valentini, G., Fernández-Oto, C., Dorigo, M. & Trianni, V. A design pattern for decentralised decision making. *PLoS ONE* **10**, e0140950, DOI: [10.1371/journal.pone.0140950](https://doi.org/10.1371/journal.pone.0140950) (2015).
27. Reina, A., Marshall, J. A. R., Trianni, V. & Bose, T. Model of the best-of-N nest-site selection process in honeybees. *Phys. Rev. E* **95**, 052411, DOI: [10.1103/PhysRevE.95.052411](https://doi.org/10.1103/PhysRevE.95.052411) (2017).
28. Cardelli, L. & Csikász-Nagy, A. The cell cycle switch computes approximate majority. *Sci. Reports* **2**, 656, DOI: [10.1038/srep00656](https://doi.org/10.1038/srep00656) (2012).
29. Cardelli, L., Hernansaiz-Ballesteros, R. D., Dalchau, N. & Csikász-Nagy, A. Efficient switches in biology and computer science. *PLOS Comput. Biol.* **13**, e1005100, DOI: [10.1371/journal.pcbi.1005100](https://doi.org/10.1371/journal.pcbi.1005100) (2017).
30. Parker, C. A. C. & Zhang, H. Cooperative decision-making in decentralized multiple-robot systems: The best-of-n problem. *IEEE/ASME Transactions on Mechatronics* **14**, 240–251 (2009).
31. Franks, N. R., Dornhaus, A., Fitzsimmons, J. P. & Stevens, M. Speed versus accuracy in collective decision making. *Proc. Royal Soc. B: Biol. Sci.* **270**, 2457–2463 (2003).
32. Couzin, I., Krause, J., Franks, N. & Levin, S. Effective leadership and decision making in animal groups on the move. *Nature* **433**, 513–516 (2005).
33. Talamali, M. S., Marshall, J. A., Bose, T. & Reina, A. Improving collective decision accuracy via time-varying cross-inhibition. In *2019 International conference on robotics and automation (ICRA)*, 9652–9659 (IEEE, 2019).
34. Franks, N. R. *et al.* Speed–cohesion trade-offs in collective decision making in ants and the concept of precision in animal behaviour. *Animal Behav.* **85**, 1233–1244 (2013).
35. Reina, A., Njougouo, T., Tuci, E. & Carletti, T. Speed-accuracy trade-offs in best-of-n collective decision making through heterogeneous mean-field modeling. *Phys. Rev. E* **109**, 054307, DOI: [10.1103/PhysRevE.109.054307](https://doi.org/10.1103/PhysRevE.109.054307) (2024).
36. Prasetyo, J., De Masi, G. & Ferrante, E. Collective decision making in dynamic environments. *Swarm Intell.* **13**, 217–243 (2019).
37. Zakir, R., Dorigo, M. & Reina, A. Miscommunication between robots can improve group accuracy in best-of-n decision-making. In *2024 IEEE/RSJ International Conference on Intelligent Robots and Systems, IROS'24*, 9014–9021, DOI: [10.1109/iros58592.2024.10802464](https://doi.org/10.1109/iros58592.2024.10802464) (IEEE, Piscataway, NJ, 2024).
38. Mobilia, M. Nonlinear q-voter model with inflexible zealots. *Phys. Rev. E* **92**, DOI: [10.1103/physreve.92.012803](https://doi.org/10.1103/physreve.92.012803) (2015).
39. Reina, A., Zakir, R., De Masi, G. & Ferrante, E. Cross-inhibition leads to group consensus despite the presence of strongly opinionated minorities and asocial behaviour. *Commun. Phys.* **6**, 236, DOI: [10.1038/s42005-023-01345-3](https://doi.org/10.1038/s42005-023-01345-3) (2023).

40. Khaluf, Y., Pinciroli, C., Valentini, G. & Hamann, H. The impact of agent density on scalability in collective systems: noise-induced versus majority-based bistability. *Swarm Intell.* **11**, 155–179, DOI: [10.1007/s11721-017-0137-6](https://doi.org/10.1007/s11721-017-0137-6) (2017).
41. Antonic, N., Zakir, R., Dorigo, M. & Reina, A. Collective robustness of heterogeneous decision-makers against stubborn individual. In *Proceedings of the 23rd International Conference on Autonomous Agents and Multiagent Systems (AAMAS 2024)*, 68–77, DOI: [10.5555/3635637.3662853](https://doi.org/10.5555/3635637.3662853) (International Foundation for Autonomous Agents and Multiagent Systems, Richland, SC, 2024).
42. De Masi, G. *et al.* Robot swarm democracy: the importance of informed individuals against zealots. *Swarm Intell.* **15**, DOI: [10.1007/s11721-021-00197-3](https://doi.org/10.1007/s11721-021-00197-3) (2021).
43. Zakir, R., Dorigo, M. & Reina, A. Robot swarms break decision deadlocks in collective perception through cross-inhibition. In Dorigo, M. *et al.* (eds.) *Swarm Intelligence*, 209–221 (Springer International Publishing, Cham, 2022).
44. Golman, R., Hagmann, D. & Miller, J. H. Polya’s bees: A model of decentralized decision-making. *Sci. Adv.* **1**, e1500253, DOI: [10.1126/sciadv.1500253](https://doi.org/10.1126/sciadv.1500253) (2015).
45. Jhawar, J. *et al.* Noise-induced schooling of fish. *Nat. Phys.* **16**, 488–493, DOI: [10.1038/s41567-020-0787-y](https://doi.org/10.1038/s41567-020-0787-y) (2020).
46. Liu, Z., Crosscombe, M. & Lawry, J. Imprecise evidence in social learning. *Swarm Intell.* **19**, 1–27, DOI: [10.1007/s11721-024-00238-7](https://doi.org/10.1007/s11721-024-00238-7) (2025).
47. Canciani, F., Talamali, M. S., Marshall, J. A. R., Bose, T. & Reina, A. Keep calm and vote on: Swarm resiliency in collective decision making. In *Proceedings of Workshop Resilient Robot Teams of the 2019 IEEE International Conference on Robotics and Automation (ICRA 2019)*, 4 (IEEE Press, Piscataway, NJ, 2019).
48. Klein, J., d’Onofrio, A. & Petrov, T. Exploring consensus robustness in swarms with disruptive individuals. In Margaria, T. & Steffen, B. (eds.) *Leveraging Applications of Formal Methods, Verification and Validation. Rigorous Engineering of Collective Adaptive Systems*, 33–48 (Springer Nature Switzerland, Cham, 2025).
49. Khalil, N., Miguel, M. S. & Toral, R. Zealots in the mean-field noisy voter model. *Phys. Rev. E* **97**, DOI: [10.1103/physreve.97.012310](https://doi.org/10.1103/physreve.97.012310) (2018).
50. Franks, N. R. *et al.* Can ant colonies choose a far-and-away better nest over an in-the-way poor one? *Animal Behav.* **76**, 323–334, DOI: [10.1016/j.anbehav.2008.02.009](https://doi.org/10.1016/j.anbehav.2008.02.009) (2008).
51. Leaf, J. & Adams, J. A. The effect of uneven and obstructed site layouts in best-of-n. *Swarm Intell.* **18**, 311–333, DOI: [10.1007/s11721-024-00236-9](https://doi.org/10.1007/s11721-024-00236-9) (2024).
52. Centola, D., Becker, J., Brackbill, D. & Baronchelli, A. Experimental evidence for tipping points in social convention. *Science* **360**, 1116–1119, DOI: [10.1126/science.aas8827](https://doi.org/10.1126/science.aas8827) (2018).
53. Couzin, I. D. *et al.* Uninformed individuals promote democratic consensus in animal groups. *Science* **334**, 1578–1580 (2011).
54. Rajendran, H., Haluts, A., Gov, N. S. & Feinerman, O. Ants resort to majority concession to reach democratic consensus in the presence of a persistent minority. *Curr. Biol.* **32**, 645–653.e8, DOI: [10.1016/j.cub.2021.12.013](https://doi.org/10.1016/j.cub.2021.12.013) (2022).

55. Marvel, S. A., Hong, H., Papush, A. & Strogatz, S. H. Encouraging moderation: Clues from a simple model of ideological conflict. *Phys. Rev. Lett.* **109**, 118702, DOI: [10.1103/PhysRevLett.109.118702](https://doi.org/10.1103/PhysRevLett.109.118702) (2012).
56. d'Amore, F. & Ziccardi, I. Phase transition of the 3-majority opinion dynamics with noisy interactions. *Theor. Comput. Sci.* **1028**, 115030, DOI: [10.1016/j.tcs.2024.115030](https://doi.org/10.1016/j.tcs.2024.115030) (2025).
57. Gillespie, D. T., Hellander, A. & Petzold, L. R. Perspective: Stochastic algorithms for chemical kinetics. *The J. chemical physics* **138** (2013).
58. Valentini, G., Brambilla, D., Hamann, H. & Dorigo, M. Collective perception of environmental features in a robot swarm. In Dorigo, M. & et al. (eds.) *Swarm Intelligence (ANTS 2016)*, vol. 9882 of *LNCS*, 65–76, DOI: [10.1007/978-3-319-44427-7_6](https://doi.org/10.1007/978-3-319-44427-7_6) (Springer, 2016).
59. Chin, K. Y., Khaluf, Y. & Pinciroli, C. Minimalistic collective perception with imperfect sensors. In *2023 IEEE/RSJ International Conference on Intelligent Robots and Systems (IROS)*, 8862–8868, DOI: [10.1109/IROS55552.2023.10341384](https://doi.org/10.1109/IROS55552.2023.10341384) (2023).
60. Ebert, J. T., Gauci, M. & Nagpal, R. Multi-feature collective decision making in robot swarms. In *Proceedings of the 17th International Conference on Autonomous Agents and MultiAgent Systems*, 1711–1719 (2018).
61. Rubenstein, M., Ahler, C., Hoff, N., Cabrera, A. & Nagpal, R. Kilobot: A low cost robot with scalable operations designed for collective behaviors. *Robotics Auton. Syst.* **62**, 966–975 (2014).
62. Antoun, A. *et al.* Kilogrid: a modular virtualization environment for the kilobot robot. In *2016 IEEE/RSJ International Conference on Intelligent Robots and Systems (IROS)*, 3809–3814 (IEEE Press, 2016).
63. Valentini, G. *et al.* Kilogrid: A novel experimental environment for the kilobot robot. *Swarm Intell.* **12**, 245–266 (2018).
64. van Kampen, N. G. *Stochastic processes in physics and chemistry* (Elsevier, Amsterdam, NL, 1992).
65. King, A. J. & Cowlshaw, G. When to use social information: the advantage of large group size in individual decision making. *Biol. Lett.* **3**, 137–139, DOI: [10.1098/rsbl.2007.0017](https://doi.org/10.1098/rsbl.2007.0017) (2007).
66. Hamann, H. & Reina, A. Scalability in computing and robotics. *IEEE Transactions on Comput.* **71**, 1453–1465, DOI: [10.1109/TC.2021.3089044](https://doi.org/10.1109/TC.2021.3089044) (2022).
67. Salahshour, M. Phase diagram and optimal information use in a collective sensing system. *Phys. Rev. Lett.* **123**, 068101, DOI: [10.1103/PhysRevLett.123.068101](https://doi.org/10.1103/PhysRevLett.123.068101) (2019).
68. Bak-Coleman, J. B. *et al.* Stewardship of global collective behavior. *Proc. Natl. Acad. Sci.* **118**, e2025764118, DOI: [10.1073/pnas.2025764118](https://doi.org/10.1073/pnas.2025764118) (2021).
69. Borofsky, T. *et al.* Hive minded: like neurons, honey bees collectively integrate negative feedback to regulate decisions. *Animal Behav.* **168**, 33–44, DOI: [10.1016/j.anbehav.2020.07.023](https://doi.org/10.1016/j.anbehav.2020.07.023) (2020).
70. Reina, A., Bose, T., Trianni, V. & Marshall, J. A. R. Effects of spatiality on value-sensitive decisions made by robot swarms. In *Distributed Autonomous Robotic Systems (DARS 2016): The 13th International Symposium*, vol. 6 of *SPAR*, 461–473 (Springer International Publishing, Cham, Switzerland, 2018).

71. Franks, N. R., Pratt, S. C., Mallon, E. B., Britton, N. F. & Sumpter, D. J. T. Information flow, opinion polling and collective intelligence in house-hunting social insects. *Philos. Transactions Royal Soc. B: Biol. Sci.* **357**, 1567–1583 (2002).
72. Taleb, N. N. 'Antifragility' as a mathematical idea. *Nature* **494**, 430–430, DOI: [10.1038/494430e](https://doi.org/10.1038/494430e) (2013).
73. Leonard, N. E., Bizyaeva, A. & Franci, A. Fast and flexible multiagent decision-making. *Annu. Rev. Control. Robotics, Auton. Syst.* **7**.
74. Gómez-Nava, L. *et al.* Fish shoals resemble a stochastic excitable system driven by environmental perturbations. *Nat. Phys.* **19**, 663–669 (2023).
75. Albani, D., IJsselmuiden, J., Haken, R. & Trianni, V. Monitoring and mapping with robot swarms for agricultural applications. In *2017 14th IEEE International Conference on Advanced Video and Signal Based Surveillance (AVSS)*, 1–6, DOI: [10.1109/AVSS.2017.8078478](https://doi.org/10.1109/AVSS.2017.8078478) (2017).
76. Nagy, M. *et al.* Synergistic benefits of group search in rats. *Curr. Biol.* **30**, 4733–4738.e4, DOI: [10.1016/j.cub.2020.08.079](https://doi.org/10.1016/j.cub.2020.08.079) (2020).
77. Sosna, M. M. G. *et al.* Individual and collective encoding of risk in animal groups. *Proc. Natl. Acad. Sci.* **116**, 20556–20561, DOI: [10.1073/pnas.1905585116](https://doi.org/10.1073/pnas.1905585116) (2019).
78. Rausch, I., Reina, A., Simoens, P. & Khaluf, Y. Coherent collective behaviour emerging from decentralised balancing of social feedback and noise. *Swarm Intell.* **13**, 321–345, DOI: [10.1007/s11721-019-00173-y](https://doi.org/10.1007/s11721-019-00173-y) (2019).
79. Strogatz, S. H. *Nonlinear Dynamics and Chaos: With Applications to Physics, Biology, Chemistry, and Engineering* (CRC Press, 2018).
80. Toral, R. & Tessone, C. J. Finite size effects in the dynamics of opinion formation. *Commun. Comput. Phys.* **2**, 177–195 (2007).
81. Biancalani, T., Dyson, L. & McKane, A. J. Noise-induced bistable states and their mean switching time in foraging colonies. *Phys. Rev. Lett.* **112**, 038101, DOI: [10.1103/PhysRevLett.112.038101](https://doi.org/10.1103/PhysRevLett.112.038101) (2014).
82. Pinciroli, C., Talamali, M. S., Reina, A., Marshall, J. A. R. & Trianni, V. Simulating Kilobots within ARGoS: models and experimental validation. In M. Dorigo *et al.* (ed.) *Swarm Intelligence (ANTS 2018)*, vol. 11172 of *LNCS*, 176–187, DOI: https://doi.org/10.1007/978-3-030-00533-7_14 (Springer, Cham, 2018).
83. Aust, T., Talamali, M., Dorigo, M., Hamann, H. & Reina, A. The hidden benefits of limited communication and slow sensing in collective monitoring of dynamic environments. In Dorigo, M. & *et al.* (eds.) *Swarm Intelligence (ANTS 2022)*, vol. 13491 of *LNCS* (Springer, 2022).

Acknowledgements

R. Zakir and M. Dorigo acknowledge support from the Belgian F.R.S.-FNRS, of which they are a FRiA Doctoral student and a Research Director, respectively. A.R. acknowledges support from DFG under Germany's Excellence Strategy - EXC 2117 - 422037984.

Author contributions statement

A.R. conceived the original idea and directed the project. R.Z, T.C, and A.R. performed the mean-field ODE analysis. R.Z and A.R performed the stochastic analysis. R.Z. designed and implemented the robot control code for the robot simulations. R.Z. generated the figures. R.Z. and A.R wrote the first draft of the paper, and all authors edited the paper.